AD-A121 399 CRT IMAGE DISTORTION DETERMINATION EXPERIMENT(U) ROME 1/1
AIR DEVELOPMENT CENTER GRIFFISS AFB NY J A SIEFFERT
SEP 82 RADC-TR-82-239

UNCLASSIFIED F/G 9/1 NL

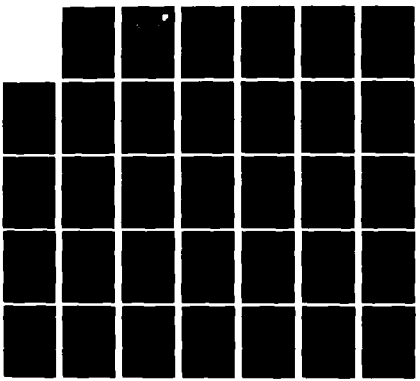

END

FILMED
DTIC

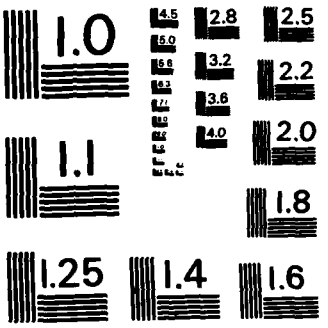

MICROCOPY RESOLUTION TEST CHART
NATIONAL BUREAU OF STANDARDS-1963-A

AD A121399

RADC-TR-82-239
In-House Report
September 1982

CRT IMAGE DISTORTION DETERMINATION EXPERIMENT

James A. Sieffert

APPROVED FOR PUBLIC RELEASE; DISTRIBUTION UNLIMITED

DTIC
ELECTE
1982
D

ROME AIR DEVELOPMENT CENTER
Air Force Systems Command
Griffiss Air Force Base, NY 13441

82 022

This report has been reviewed by the RADC Public Affairs Office (PA) and is releasable to the National Technical Information Service (NTIS). At NTIS it will be releasable to the general public, including foreign nations.

RADC-TR-82-239 has been reviewed and is approved for publication.

APPROVED:

GEORGE R. HUGHES
Assistant Chief
Image Systems Branch

APPROVED:

JOHN N. ENTZMINGER, JR.
Technical Director
Intelligence and Reconnaissance Division

FOR THE COMMANDER:

JOHN P. HUSS
Acting Chief, Plans Office

If your address has changed or if you wish to be removed from the RADC mailing list, or if the addressee is no longer employed by your organization, please notify RADC (IRRA) Griffiss AFB NY 13441. This will assist us in maintaining a current mailing list.

Do not return copies of this report unless contractual obligations or notices on a specific document requires that it be returned.

UNCLASSIFIED

SECURITY CLASSIFICATION OF THIS PAGE (When Data Entered)

REPORT DOCUMENTATION PAGE		READ INSTRUCTIONS BEFORE COMPLETING FORM
1. REPORT NUMBER RADC-TR-82-239	2. GOVT ACCESSION NO. AD-A121399	3. RECIPIENT'S CATALOG NUMBER
4. TITLE (and Subtitle) CRT IMAGE DISTORTION DETERMINATION EXPERIMENT		5. TYPE OF REPORT & PERIOD COVERED In-House Report May 80 - Feb 82
		6. PERFORMING ORG. REPORT NUMBER N/A
7. AUTHOR(s) James A. Sieffert		8. CONTRACT OR GRANT NUMBER(s) N/A
9. PERFORMING ORGANIZATION NAME AND ADDRESS Rome Air Development Center (IRRA) Griffiss AFB NY 13441		10. PROGRAM ELEMENT, PROJECT, TASK AREA & WORK UNIT NUMBERS 62702F 45941734
11. CONTROLLING OFFICE NAME AND ADDRESS Rome Air Development Center (IRRA) Griffiss AFB NY 13441		12. REPORT DATE September 1982 13. NUMBER OF PAGES 52
14. MONITORING AGENCY NAME & ADDRESS (if different from Controlling Office) Same		15. SECURITY CLASS. (of this report) UNCLASSIFIED 15a. DECLASSIFICATION/DOWNGRADING SCHEDULE N/A

16. DISTRIBUTION STATEMENT (of this Report)

Approved for public release; distribution unlimited.

17. DISTRIBUTION STATEMENT (of the abstract entered in Block 20, if different from Report)

Same

18. SUPPLEMENTARY NOTES

None

19. KEY WORDS (Continue on reverse side if necessary and identify by block number)

Photogrammetry
CRT Distortion
Camera Calibration
Sensor Calibration
Exterior Orientation

20. ABSTRACT (Continue on reverse side if necessary and identify by block number)

An analytical photogrammetric approach was used to determine the geometric distortions of cursor coordinates on an image viewing and measuring system which included a television camera, the associated electronics and a cathode ray tube display. Computer programs were developed to provide the determination of common lens distortion parameters, the camera orientation and additional distortions due to the electronic components, all in several combinations. Measurements made with the use of a calibrated

DD FORM 1 JAN 73 1473 EDITION OF 1 NOV 65 IS OBSOLETE

UNCLASSIFIED

SECURITY CLASSIFICATION OF THIS PAGE (When Data Entered)

grid were processed through a least squares solution. The mathematical formulation of the various error types can be used to determine the respective errors completely, but not in a single simultaneous solution. Independent determinations of electronic distortion and camera position must be used and coordinate mensuration errors should be monitored and minimized.

TABLE OF CONTENTS

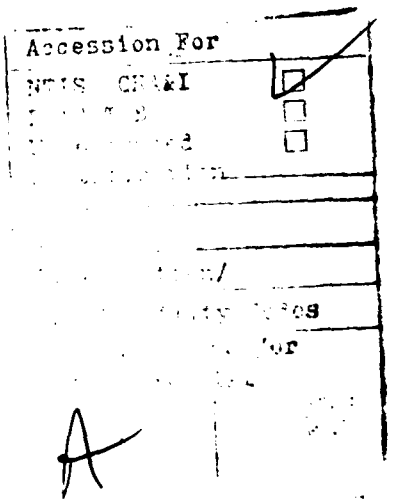

DTIC COPY INSPECTED

PREFACE

This paper presents the results of an examination of a method of arriving at values describing geometric distortions in a displayed CRT image. A rigorous procedure was tested which combines the traditional photogrammetric distortion and orientation solutions with electronic distortions particular to CRT viewing and display systems.

INTRODUCTION

An analytical photogrammetric approach was used to determine the geometric distortions of cursor coordinates on an image viewing and measuring system which included a television camera, the associated electronics and a cathode ray tube display. Computer programs were developed to provide the determination of common lens distortion parameters, the camera orientation and additional distortions due to the electronic components, all in several combinations. Measurements made with the use of a calibrated grid were processed through a least squares solution.

The similarities between a frame photogrammetric camera and a TV camera allow the application of photogrammetric principles to the TV image. Both systems use an optical lens to focus the image of a real object onto an imaging medium which is used to determine the spatial characteristics of the object. Electron lenses and magnetic lenses, as they are commonly employed by television systems, exhibit many of the distortion forms found in optical lens systems although they may have different causes. Successful analysis of television systems photogrammetrically for the determination of accuracy and distortion has taken place since 1968. The sources and patterns of distortions were derived for the various components of spacecraft television systems. These systems included return-beam vidicon cameras used for earth resources evaluation, weather monitoring, lunar mapping and martian observation.

The product of the investigation was to be a mathematical procedure for determining geometric distortion and an estimation of the significance of the input image point placement and

environmental variation from the measured variances without an attempt to separate any specific internal hardware influence sources.

The necessity of acquiring accurate and precise coordinate measurements of photographic images in photogrammetry has prompted extensive research into the investigation of the causes and correction of error in the image recording and mensuration process. The causes of positional error in a photographic system may be divided into two broad categories: defects arising from optical sources; and those caused by deformation of the imaging material. Any influence which causes, in effect, a bending of the theoretically straight line connecting an object to its ideal photographic position (collinearity) is an error for which a systematic correction would be beneficial.

TECHNICAL DISCUSSION

Error Sources and Mathematical Approximation

A typical precision television system camera contains a reseau which is etched onto the cathode target plate of the vidicon or orthicon camera tube which is measured accurately prior to assembly. During subsequent operation of the camera, light is focused onto the target plate through the camera lens. A scanning electron beam, focused by magnetic coils scans the optical image and the etched reseau grid simultaneously and delivers a video signal. The electrical hardware amplifies the video signal and converts it into a radio signal which can then be transmitted, or in the case of a closed circuit system, the video signal can be sent directly to a display. The video image can be measured through the use of an electronically generated cursor. Through this process the image is sent through two optical lenses, a number of electronic lenses and electronic components.

The majority of the distortions typical in closed circuit television systems are identical in form to those encountered by photogrammetrists in common metric camera systems. The optical lens, electronic lens and magnetic lens systems in a television system exhibit similar forms of radial and tangential distortion.

The optical lens contributes all types of radial and tangential distortions which are a result of imperfect design, fabrication and centering of lens elements.

The magnetic and electron lenses together with typical CRT geometry, camera tube geometry and the electromagnetic

environment produce the same distortions due to non-uniform deflection fields, fringe field effects, screen curvature, external fields, lateral deflection at the camera tube and imperfect synchronization.

Two other forms of image warping are common in television systems. One is called trapezoidal and the other is stretch or compression distortion. The two are related and each can manifest themselves in the x and y directions. The four forms are actually scale changes in x and y coordinates as a function of x and y directions and y and x directions respectively as shown in the figures below.

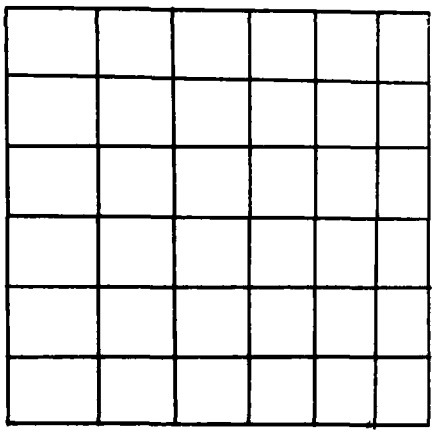

X Compression Distortion - The scale of X coordinates varies uniformly in the direction of the X axis.

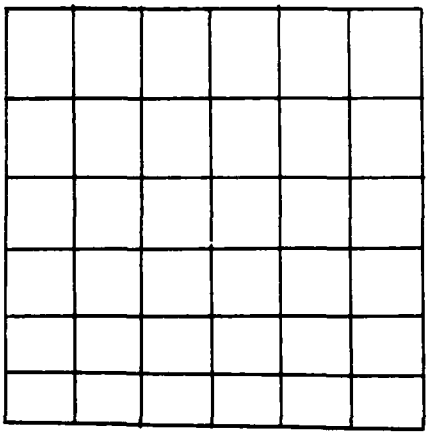

Y Compression Distortion - The scale of Y coordinates varies uniformly in the direction of the Y axis.

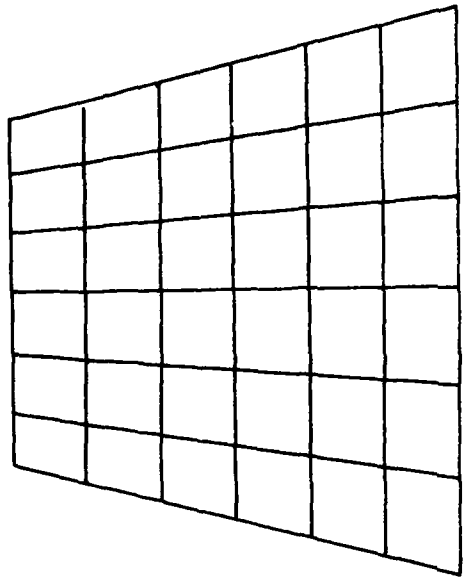

Y Trapezoidal Distortion - The scale of Y coordinates varies uniformly in the direction of the X axis.

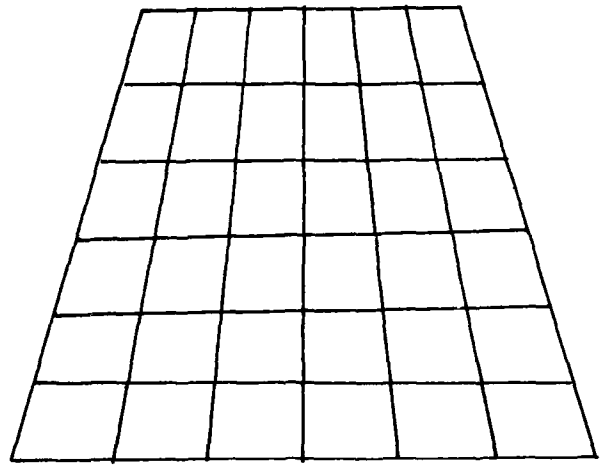

X Trapezoidal Distortion - The scale of X coordinates varies uniformly in the direction of the Y axis.

It is obvious that specific combinations of these distortions will simulate a perspective view which might be corrected by an adjustment to two of the orientation angles of the camera. This kind of combination is shown below.

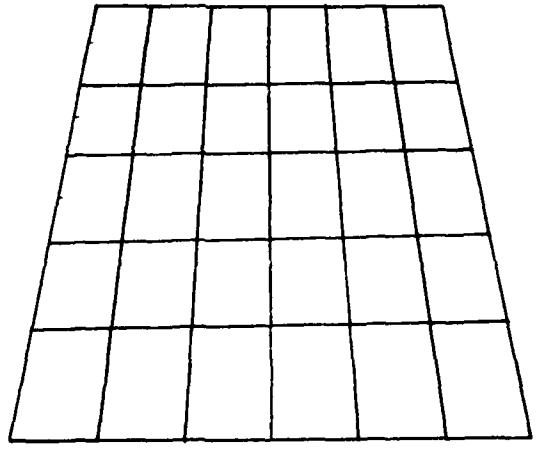

Composite distortion equations were formulated which serve to combine the radial distortions of the lens and electronics and treat them together in a least squares numerical solution. All the distortions are solved for simultaneously using polynomial formulae used in photogrammetry for optical distortions. Also included are the standard photogrammetric parameters defining the orientation of the camera. The equations were formulated in this way:

Symmetric Radial Distortion:

$$(\Delta\bar{x})_{sr} = \bar{x}\,(l_1 \cdot r^2 + l_2 \cdot r^4 + l_3 \cdot r^6 + \ldots)$$

$$(\Delta\bar{y})_{sr} = \bar{y}\,(l_1 \cdot r^2 + l_2 \cdot r^4 + l_3 \cdot r^6 + \ldots)$$

Symmetric Tangential Distortion:

$$(\Delta\bar{x})_{st} = -\bar{y}\,(q_1 \cdot r^3 + q_2 \cdot r^5 + q_3 \cdot r^7 + \ldots)$$

$$(\Delta\bar{y})_{st} = \bar{x}\,(q_1 \cdot r^3 + q_2 \cdot r^5 + q_3 \cdot r^7 + \ldots)$$

Asymmetric Radial and Tangential Distortion:

$$(\Delta\bar{x})_a = -(a_1 \cdot r^2 + a_2 \cdot r^4 + a_3 \cdot r^6 + \ldots) \sin\theta$$

$$(\Delta\bar{y})_a = (a_1 \cdot r^2 + a_2 \cdot r^4 + a_3 \cdot r^6 + \ldots) \cos\theta$$

Projective Equations:

$$\Delta\bar{x} = \frac{-f \cdot (\, m11(X-Xo) + m12(Y-Yo) + m13(Z-Zo)\,)}{(\, m31(X-Xo) + m32(Y-Yo) + m33(Z-Zo)\,)} + xp - \bar{x}$$

$$\Delta\bar{y} = \frac{-f \cdot (\, m21(X-Xo) + m22(Y-Yo) + m23(Z-Zo)\,)}{(\, m31(X-Xo) + m32(Y-Yo) + m33(Z-Zo)\,)} + yp - \bar{y}$$

Composite Electronic Distortions:

$$(\Delta\bar{x})_e = d \cdot \bar{x} \cdot \bar{y} + e \cdot \bar{x}^2 + h$$

$$(\Delta\bar{y})_e = k \cdot \bar{x} \cdot \bar{y} + n \cdot \bar{y}^2 + s$$

The expressions $(\Delta\bar{x})sr$ $(\Delta\bar{y})sr$, $(\Delta\bar{x})st$ $(\Delta\bar{y})st$, and $(\Delta\bar{x})a$ $(\Delta\bar{y})a$ are the corrections to the measured photocoordinates for symmetric radial, symmetric tangential and asymmetrical tangential and radial distortions respectively in the x and y directions respectively.

The projective equations of photogrammetry are given where: the parameters mij represent the elements of the orientation matrix; X, Y and Z are the true object coordinates; Xo, Yo, and Zo define the camera position in space; xp and yp define the principal point position; x and y are the photocoordinates of the target points corrected for camera orientation and position with no distortions or deformations; and r is the distance between the principal point and an image point.

If these equations are each applied in a distortion of a square grid pattern, the resulting patterns may appear like these:

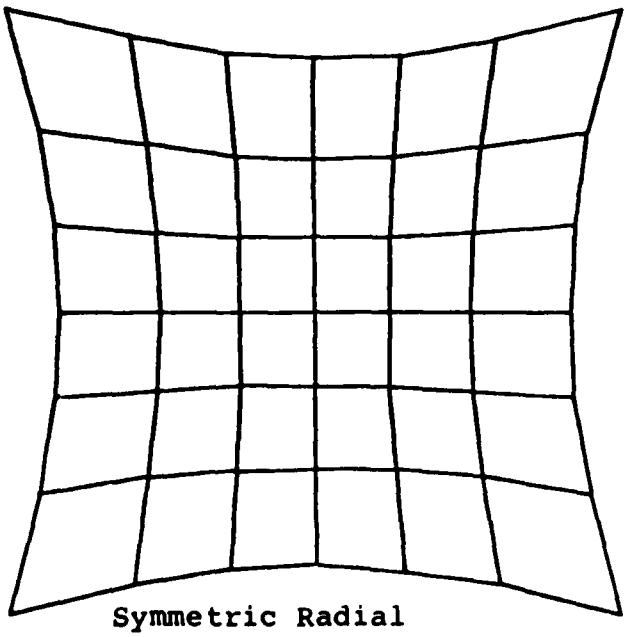

Symmetric Radial

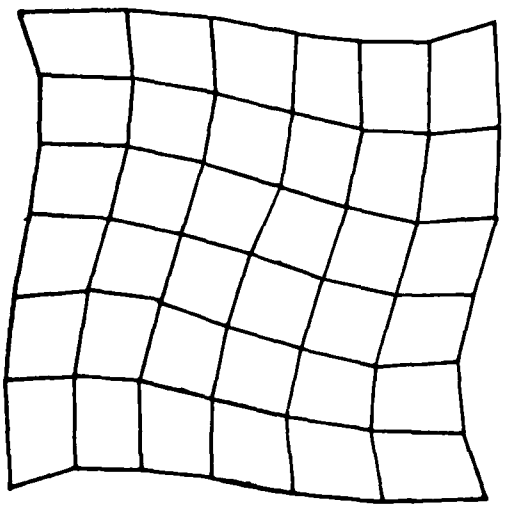

Symmetric Tangential

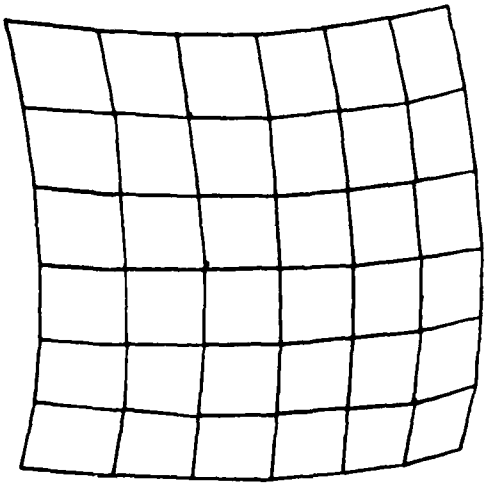

Asymmetric

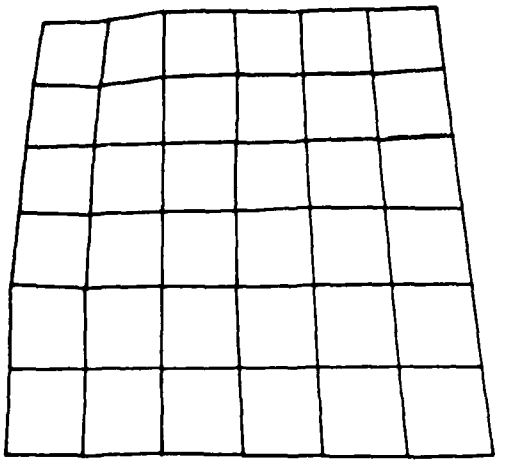

Projective

If the equations are all applied to the distortion of one grid, a composite pattern will appear like this:

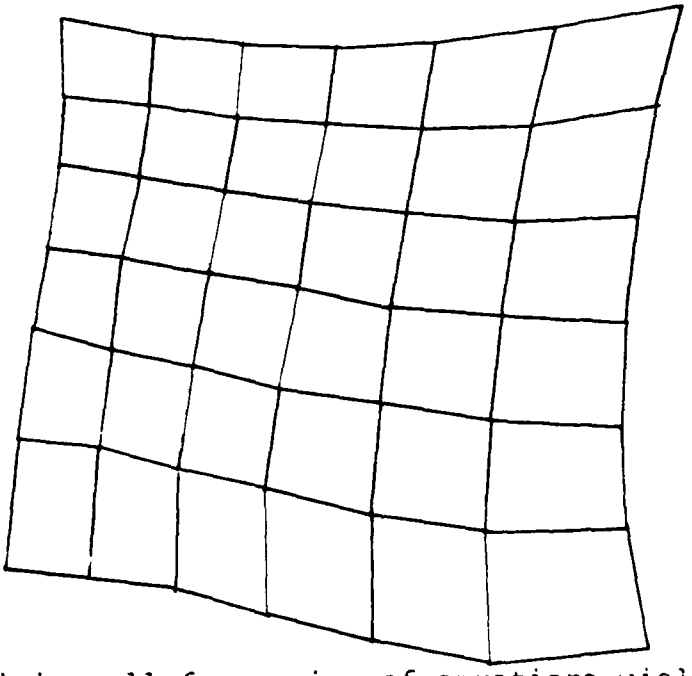

Combining all four pairs of equations yields two observation equations:

$$e_x = \bar{x} + (\Delta\bar{x})_{sr} + (\Delta\bar{x})_{st} + (\Delta\bar{x})_{a} + (\Delta\bar{x})_{e} - x = 0$$

$$e_y = y + (y)_{sr} + (y)_{st} + (y)_a + (y)_e - y = 0$$

Through a least squares determination, where each known and measured reseau point provides two observation equations, the parameters which define the radial and tangential distortions and orientation can be found. The equations rectify the image by removing distortions which occur between the imaging of the etched reseau and the measurement of the coordinates of the displayed CRT image.

EXPERIMENTATION

Overall Process

The purpose of the study undertaken here was to evaluate a method for identifying the systematic geometric distortions present in a closed circuit TV coordinate display. Final expected x and y coordinate accuracies will be defined to establish a relationship between normally obtainable coordinates and actual calibrated coordinates.

Target glass grids were measured by comparator to establish calibrated coordinate values for each target. An operator performed independent measurements using the calibrated grids displayed through the system.

Programs were written to solve simultaneous observation equations for four combinations of distortions to be compared: lens, projective and electronic; lens and projective; lens and electronic; and electronic only. A least squares approach iterates to a solution for which the sum of the residual distance squared between the calibrated and computed coordinates will be a minimum.

To test and evaluate the distortion formulae and programs for correctness, accuracy and feasibility, several ficticious data sets containing all the distortions in various combinations were computed and applied. The ficticious data was used to test for proper formulation and debugging and each set of actual data was applied to every solution method.

Analysis of variance routines were used to assess the significance of outside influences upon measurement such as

operators, target point placement within the image and measurement sets.

Experimental Procedure

The chosen target shape was a circular dot. Three grids were constructed on a clear glass plate consisting of 49 points each in seven rows and seven columns. The grids had intervals of 5, 10 and 15mm respectively, giving complete dimensions of 30, 60 and 90mm. The dot sizes were directly proportional to the grid dimensions. The three grids differed only in scale. Their dimensions are summarized in the following table.

Calibrated Grid Characteristics

Grid Description	Grid Interval, mm	Total Dimensions, mm	Target Size, mm
small	5	30 x 30	0.25
medium	10	60 x 60	0.5
large	15	90 x 90	0.75

The grids were measured on a comparator with a least reading of 1 micron and final calibrated coordinates were assigned the average of three pointings.

The measurements on the system were made with four factors varying: 2 coordinate directions (x and y); 5 setups (5 different grids and camera setup combinations); 7 rows of targets and 7 columns of targets.

The operator measured each setup-grid combination once giving a total of 5 measurement sets, each consisting of 49 points, all with 9 pointings on each target. One pointing consisted of one x and one y measurement. A total of 245 points were measured by a total of 2195 pointings for 5 complete grid measurement sets.

In each measurement set of 49 points, the target points were measured in random order. The CRT screen illumination, displayed target size and room temperature were kept constant throughout the experiment.

Data Analysis

Four sets of 49 ficticious x and y coordinate pairs were generated to model the four distortion combinations of lens-projective-electronic, lens projective, lens-electronic and electronic. A 7 x 7 point grid with coordinates in increments of 10 mm was used for the computation of the changes in x and y from the lens and electronic distortions. These were added to the original coordinates and the resulting values were input as photocoordinates in an analytical projective routine for which the orientation was given.

The formulae used to compute the coordinate changes are shown below. The final output ground coordinates were then used as true calibrated coordinates and the original nominal coordinates were treated as measured coordinates in the testing of the solution programs.

Lens Distortions

Symmetric Radial:

$$\Delta\bar{x} = \bar{x}(l_1 \cdot r^2 + l_2 \cdot r^4)$$

$$\Delta\bar{y} = \bar{y}(l_1 \cdot r^2 + l_2 \cdot r^4)$$

Symmetric Tangential:

$$\Delta\bar{x} = -\bar{y}(q_1 \cdot r + q_2 \cdot r^3)$$

$$\Delta\bar{y} = \bar{x}(q_1 \cdot r + q_2 \cdot r^3)$$

Asymmetric:

$$\Delta\bar{x} = -(a_1 \cdot r^2 + a_2 \cdot r^4) \sin\theta$$

$$\Delta\bar{y} = (a_1 \cdot r^2 + a_2 \cdot r^4) \cos\theta$$

Projective Distortions

$$\Delta\bar{x} = Xo - (Zj-Zo) \cdot \frac{(m11 \cdot A + m12 \cdot B + m13 \cdot C)}{(m31 \cdot A + m32 \cdot B + m33 \cdot C)} - \bar{x}$$

$$\Delta\bar{y} = Yo - (Zj-Zo) \cdot \frac{(m21 \cdot A + m22 \cdot B + m23 \cdot C)}{(m31 \cdot A + m32 \cdot B + m33 \cdot C)} - \bar{y}$$

Where A = X - Xo, B = Y - Yo, C = Z - Zo and mij = an element of the orientation matrix.

Electronic Distortions

X Trapezoidal:	$\Delta\bar{x} = d \cdot \bar{x} \cdot \bar{y}$	$\Delta\bar{y} = 0$
Y Trapezoidal:	$\Delta\bar{x} = 0$	$\Delta\bar{y} = k \cdot \bar{x} \cdot \bar{y}$
X Compression:	$\Delta\bar{x} = e \cdot \bar{x}^2 + h$	$\Delta\bar{y} = 0$
Y Compression:	$\Delta\bar{x} = 0$	$\Delta\bar{y} = n \cdot \bar{y}^2 + s$

The distortion equations above were combined to form two observation equations which define the relationship between the true image coordinates and the measured CRT coordinates:

$$E_x = \bar{x} + \bar{x}(l_1 \cdot r^2 + l_2 \cdot r^4) - \bar{y}(q_1 \cdot r + q_2 \cdot r^3) -$$

$$\sin\Theta\,(a_1 \cdot r^2 + a_2 \cdot r^4) + f \cdot \frac{(\,m11(X-Xo) + m12(Y-Yo) + m13(Z-Zo)\,)}{(\,m31(X-Xo) + m32(Y-Yo) + m33(Z-Zo)\,)}$$

$$+ d \cdot \bar{x} \cdot \bar{y} + e \cdot \bar{x}^2 + h = 0$$

$$E_y = \bar{y} + \bar{y}(l_1 \cdot r^2 + l_2 \cdot r^4) - \bar{x}(q_1 \cdot r + q_2 \cdot r^3) -$$

$$\cos\Theta\,(a_1 \cdot r^2 + a_2 \cdot r^4) + f \cdot \frac{(\,m21(X-Xo) + m22(Y-Yo) + m23(Z-Zo)\,)}{(\,m31(X-Xo) + m32(Y-Yo) + m33(Z-Zo)\,)}$$

$$+ k \cdot \bar{x} \cdot \bar{y} + n \cdot \bar{y}^2 + s = 0$$

The unknown parameters are: l1, l2, q1, q2, O, a1, a2, K, O, W, Xo, Yo, Zo, d, e, h, k, n and s. The observation equations were linearized in order to be applicable to a least squares solution to obtain corrections for successive approximations of the unknowns.

If the observation equations above are expanded by Taylor's series and all second and higher order terms are neglected, they are linearized. These partial derivatives of the observation equations with respect to the unknown parameters are shown on the following three pages.

If n calibrated points are known, a total of n pairs of equations can be used. A minimium of 10 points are required for a complete solution. A least squares solution has as its basis the condition that V WV is minimized where V contains the adjustment residuals and W is the weight matrix.

The least squares iterative solution computes successive corrections to the unknown parameter approximations by solving the following matrix equation for the correction vector:

$$\delta = - \left[B^T WB\right]^{-1} x \left[B^T WE\right]$$

Where B is the partial derivative matrix computed from the latest approximations. New corrections are computed and applied to the approximations until the sum of the squares of the residuals stabilizes at a minimum value.

$$\frac{\partial Ex}{\partial l1} = x \cdot r^{2} \qquad \frac{\partial Ex}{\partial l2} = x \cdot r^{4} \qquad \frac{\partial Ex}{\partial q1} = -y \cdot r \qquad \frac{\partial Ex}{\partial q2} = -y \cdot r^{3}$$

$$\frac{\partial Ex}{\partial \theta} = -\cos\theta (a_1 \cdot r^{2} + a_2 \cdot r^{4}) \qquad \frac{\partial Ex}{\partial \theta} = -\sin\theta \cdot r^{2} \qquad \frac{\partial Ex}{\partial \theta} = -\sin\theta \cdot r^{4}$$

$$\frac{\partial Ex}{\partial K} = \frac{-f \cdot A}{C \cdot C}\left[\frac{\partial m31}{\partial K}(X-Xo) + \frac{\partial m32}{\partial K}(Y-Yo) + \frac{\partial m33}{\partial K}(Z-Zo)\right] + \frac{f}{C}\left[\frac{\partial m11}{\partial K}(X-Xo) + \frac{\partial m12}{\partial K}(Y-Yo) + \frac{\partial m13}{\partial K}(Z-Zo)\right]$$

$$\frac{\partial Ex}{\partial \phi} = \frac{-f \cdot A}{C \cdot C}\left[\frac{\partial m31}{\partial \phi}(X-Xo) + \frac{\partial m32}{\partial \phi}(Y-Yo) + \frac{\partial m33}{\partial \phi}(Z-Zo)\right] + \frac{f}{C}\left[\frac{\partial m11}{\partial \phi}(X-Xo) + \frac{\partial m12}{\partial \phi}(Y-Yo) + \frac{\partial m13}{\partial \phi}(Z-Zo)\right]$$

$$\frac{\partial Ex}{\partial w} = \frac{-f \cdot A}{C \cdot C}\left[\frac{\partial m31}{\partial w}(X-Xo) + \frac{\partial m32}{\partial w}(Y-Yo) + \frac{\partial m33}{\partial w}(Z-Zo)\right] + \frac{f}{C}\left[\frac{\partial m11}{\partial w}(X-Xo) + \frac{\partial m12}{\partial w}(Y-Yo) + \frac{\partial m13}{\partial w}(Z-Zo)\right]$$

$$\frac{\partial Ex}{\partial Xo} = \frac{-f}{C}(m31 \cdot A + m11 \cdot C) \qquad \frac{\partial Ex}{\partial Yo} = \frac{-f}{C}(m32 \cdot A + m12 \cdot C) \qquad \frac{\partial Ex}{\partial Zo} = \frac{-f}{C}(m33 \cdot A + m13 \cdot C)$$

$$\frac{\partial Ex}{\partial d} = x \cdot y \qquad \frac{\partial Ex}{\partial e} = x^{2} \qquad \frac{\partial Ex}{\partial h} = 1 \qquad \frac{\partial Ex}{\partial k} = 0 \qquad \frac{\partial Ex}{\partial n} = 0 \qquad \frac{\partial Ex}{\partial s} = 0$$

$$\frac{\partial Ey}{\partial l1} = y \cdot r^2 \qquad \frac{\partial Ey}{\partial l2} = y \cdot r^4 \qquad \frac{\partial Ey}{\partial q1} = x \cdot r \qquad \frac{\partial Ey}{\partial q2} = x \cdot r^3$$

$$\frac{\partial Ey}{\partial \theta} = -\sin\theta(a_1 \cdot r^2 + a_2 \cdot r^4) \qquad \frac{\partial Ey}{\partial \theta} = \cos\theta \cdot r^2 \qquad \frac{\partial Ey}{\partial \theta} = \cos\theta \cdot r^4$$

$$\frac{\partial Ey}{\partial K} = \frac{-f \cdot A}{C \cdot C}\left[\frac{\partial m31}{\partial K}(X-Xo) + \frac{\partial m32}{\partial K}(Y-Yo) + \frac{\partial m33}{\partial K}(Z-Zo)\right] + \frac{f}{C}\left[\frac{\partial m21}{\partial K}(X-Xo) + \frac{\partial m22}{\partial K}(Y-Yo) + \frac{\partial m23}{\partial K}(Z-Zo)\right]$$

$$\frac{\partial Ey}{\partial \phi} = \frac{-f \cdot A}{C \cdot C}\left[\frac{\partial m31}{\partial \phi}(X-Xo) + \frac{\partial m32}{\partial \phi}(Y-Yo) + \frac{\partial m33}{\partial \phi}(Z-Zo)\right] + \frac{f}{C}\left[\frac{\partial m21}{\partial \phi}(X-Xo) + \frac{\partial m22}{\partial \phi}(Y-Yo) + \frac{\partial m23}{\partial \phi}(Z-Zo)\right]$$

$$\frac{\partial Ey}{\partial w} = \frac{-f \cdot A}{C \cdot C}\left[\frac{\partial m31}{\partial w}(X-Xo) + \frac{\partial m32}{\partial w}(Y-Yo) + \frac{\partial m33}{\partial w}(Z-Zo)\right] + \frac{f}{C}\left[\frac{\partial m21}{\partial w}(X-Xo) + \frac{\partial m22}{\partial w}(Y-Yo) + \frac{\partial m23}{\partial w}(Z-Zo)\right]$$

$$\frac{\partial Ey}{\partial Xo} = \frac{-f}{C}(m31 \cdot A + m21 \cdot C) \qquad \frac{\partial Ey}{\partial Yo} = \frac{-f}{C}(m32 \cdot A + m22 \cdot C) \qquad \frac{\partial Ey}{\partial Zo} = \frac{-f}{C}(m33 \cdot A + m23 \cdot C)$$

$$\frac{\partial Ey}{\partial d} = 0 \qquad \frac{\partial Ey}{\partial e} = 0 \qquad \frac{\partial Ey}{\partial h} = 0 \qquad \frac{\partial Ey}{\partial k} = x \cdot y \qquad \frac{\partial Ey}{\partial n} = y^2 \qquad \frac{\partial Ey}{\partial s} = 1$$

The orientation matrix M:

$$\begin{bmatrix} \cos\phi\cos K & \cos w\sin K + \sin w\sin\phi\cos K \\ -\cos\phi\sin K & \cos w\cos K - \sin w\sin\phi\sin K \\ \sin\phi & -\sin w\cos\phi \end{bmatrix}$$

$$\begin{bmatrix} \sin w\sin K - \cos w\sin\phi\cos K \\ \sin w\cos K + \cos w\sin\phi\sin K \\ \cos\phi\cos w \end{bmatrix}$$

$$\frac{\partial M}{\partial K} = \begin{bmatrix} m21 & m22 & m23 \\ -m11 & -m12 & -m13 \\ 0 & 0 & 0 \end{bmatrix} \qquad \frac{\partial M}{\partial w} = \begin{bmatrix} 0 & -m13 & m12 \\ 0 & -m23 & m22 \\ 0 & -m33 & m32 \end{bmatrix}$$

$$\frac{\partial M}{\partial \phi} = \begin{bmatrix} -\sin\phi\cos K & m11\cdot\sin w & -m11\cdot\cos w \\ \sin\phi\sin K & m21\cdot\sin w & -m21\cdot\cos w \\ \cos\phi & m31\cdot\sin w & -m31\cdot\cos w \end{bmatrix}$$

$$A = m11(X-Xo) + m12(Y-Yo) + m13(Z-Zo)$$

and $$B = m21(X-Xo) + m22(Y-Yo) + m23(Z-Zo)$$

$$C = m31(X-Xo) + m32(Y-Yo) + m33(Z-Zo)$$

Two observation equations resulting from one known object point can be represented in matrix form:

$$\begin{bmatrix} V_x \\ V_y \end{bmatrix} + \begin{bmatrix} \frac{\partial Ex}{\partial l1} & \frac{\partial Ex}{\partial l2} & \frac{\partial Ex}{\partial q1} & \frac{\partial Ex}{\partial q2} & \frac{\partial Ex}{\partial \Theta} & \frac{\partial Ex}{\partial a1} & \frac{\partial Ex}{\partial a2} & \frac{\partial Ex}{\partial K} & \frac{\partial Ex}{\partial \Phi} & \frac{\partial Ex}{\partial w} & \frac{\partial Ex}{\partial Xo} \\ \frac{\partial Ey}{\partial l1} & \frac{\partial Ey}{\partial l2} & \frac{\partial Ey}{\partial q1} & \frac{\partial Ey}{\partial q2} & \frac{\partial Ey}{\partial \Theta} & \frac{\partial Ey}{\partial a1} & \frac{\partial Ey}{\partial a2} & \frac{\partial Ey}{\partial K} & \frac{\partial Ey}{\partial \Phi} & \frac{\partial Ey}{\partial w} & \frac{\partial Ey}{\partial Xo} \end{bmatrix}$$

$$\begin{bmatrix} \frac{\partial Ex}{\partial Yo} & \frac{\partial Ex}{\partial Zo} & \frac{\partial Ex}{\partial d} & \frac{\partial Ex}{\partial e} & \frac{\partial Ex}{\partial h} & \frac{\partial Ex}{\partial k} & \frac{\partial Ex}{\partial n} & \frac{\partial Ex}{\partial s} \\ \frac{\partial Ey}{\partial Yo} & \frac{\partial Ey}{\partial Zo} & \frac{\partial Ey}{\partial d} & \frac{\partial Ey}{\partial e} & \frac{\partial Ey}{\partial h} & \frac{\partial Ey}{\partial k} & \frac{\partial Ey}{\partial n} & \frac{\partial Ey}{\partial s} \end{bmatrix} \times \begin{bmatrix} \Delta l1 \\ \Delta l2 \\ \Delta q1 \\ \Delta q2 \\ \Delta \Theta \\ \Delta a1 \\ \Delta a2 \\ \Delta K \\ \Delta \Phi \\ \Delta w \\ \Delta Xo \\ \Delta Yo \\ \Delta Zo \\ \Delta d \\ \Delta e \\ \Delta h \\ \Delta k \\ \Delta n \\ \Delta s \end{bmatrix} + \begin{bmatrix} Ex \\ Ey \end{bmatrix} = \begin{bmatrix} 0 \\ 0 \end{bmatrix}$$

A full 19 parameter solution was programmed following the description above. Three other programs were written which solved for: 13 unknown parameters for lens and projection; 13 for lens and electronic; and 6 for electronic distortions only. These are subsets of the 19 parameter solution. After testing with ficticious data a 17 parameter solution was written to eliminate computation of the constants of electronic distortion, but the coefficient routine was significantly poorer than the other four and thus was not used any further.

Before the four solution methods were applied to the six measurement sets the raw measurement means were rectified for x and y scaling, translation and rotation by an affine transformation. Each set was processed by each distortion routine for a total of 24 solutions for the actual distortions. The 24 solutions were given 49 known control points.

Each target pointing variance was computed for the ANOVA analysis. The log of the variance values were input for a four-way ANOVA classification for levels of: coordinates (2), rows (7), columns (7) and setups(5). An ANOVA table was produced, F ratios were computed and tested at significance levels of 0.01 and 0.05.

The null hypothesis stated that no significant difference between parameters or interactions existed at the levels tested. Rejection of the null hypothesis when it is true is a type I error. A type I error might have ocurred one or five times in 100 if significance was found at each significance level.

A multiple range test was performed on the sample means to determine where significant differences existed among those effects which were found to be significant by the F test.

If k random sample of size n are found, the range of any subset of p sample means must exceed the least significant range before any of the means can be assumed to be different. The least significant range is denoted by $Rp = rp\sqrt{(s \div n)}$.

A full 19 parameter solution was programmed following the description above. Three other programs were written which solved for: 13 unknown parameters for lens and projection; 13 for lens and electronic; and 6 for electronic distortions only. These are subsets of the 19 parameter solution. After testing with ficticious data a 17 parameter solution was written to eliminate computation of the constants of electronic distortion, but the coefficient routine was significantly poorer than the other four and thus was not used any further.

Before the four solution methods were applied to the six measurement sets the raw measurement means were rectified for x and y scaling, translation and rotation by an affine transformation. Each set was processed by each distortion routine for a total of 24 solutions for the actual distortions. The 24 solutions were given 49 known control points.

Each target pointing variance was computed for the ANOVA analysis. The log of the variance values were input for a four-way ANOVA classification for levels of: coordinates (2), rows (7), columns (7) and setups(5). An ANOVA table was produced, F ratios were computed and tested at significance levels of 0.01 and 0.05.

The null hypothesis stated that no significant difference between parameters or interactions existed at the levels tested. Rejection of the null hypothesis when it is true is a type I error. A type I error might have ocurred one or five times in 100 if significance was found at each significance level.

A multiple range test was performed on the sample means to determine where significant differences existed among those effects which were found to be significant by the F test.

If k random sample of size n are found, the range of any subset of p sample means must exceed the least significant range before any of the means can be assumed to be different. The least significant range is denoted by $Rp = rp\sqrt{(s \div n)}$.

RESULTS

Ficticious Testing

The overall ficticious results are represented in the following table by the sum of squares of residuals in x and y for each least squares solution. The largest sum of residuals squared was observed in the 17 parameter solution and is the only one large enough not to be caused by roundoff error in the calibrated coordinates. The photocoordinates had been rounded to the nearest 0.1 micron before input.

		RESIDUALS			
Solution Type and Distortions Used	Final SSR	Total X, mm	Total Y, mm	Avg X, mm under	Avg Y, mm under
Lens, Orientation + Electronic (19)	8×10^{-8}	0.0003	0.0001	0.000053	0.000051
Lens, Orientation + Electronic (17)	191×10^{-8}	0.0052	0.0053	0.00012	0.00012
Lens and Orientation (13)	6×10^{-8}	0.0001	0.0	0.000051	0.000050
Lens and Electronic (13)	9×10^{-8}	0.0007	0.0001	0.000057	0.000051
Electronic (6)	6×10^{-8}	0.0	0.0	0.000050	0.000050

Each method was forced through 4 iterations and then allowed to stop upon minimization. All were given the same approximations and did converge very rapidly. The following tables contain the standard deviations of the unknowns from the variance-covariance matrix and the percent error in the final

Ficticious Solution Standard Deviation and Precent Error

Variable	19 Parameters		17 Parameters	
	Std. Dev.	% Error	Std. Dev.	% Error
l1	0.0	0.055	0.0	0.245 *
l2	0.0	0.045	0.0	0.0
q1	0.0	0.016	0.0	0.02
q2	0.0	0.022	0.0	0.022
θ	0.000062	0.001	0.000284	0.009
a1	0.0	0.004	0.0	0.012
a2	0.0	0.005	0.0	0.242 *
K	0.000002	0.009	0.000008	0.087 *
ϕ	0.000019	0.023	0.000058	0.708 ***
W	0.000025	1.106 *	0.0001	15.71 ***
Xo	0.000997	-0.0074	0.002036	0.036 ***
Yo	0.001258	0.0051	0.003510	0.0057 ***
Zo	0.000036	0.0	0.000146	0.002
d	0.000001	0.028	0.000003	4.48 ***
e	0.0	0.026	0.000002	0.866 ***
h	0.00097	2.56 *		
k	0.0	0.036	0.000002	0.85 ***
n	0.0	0.033	0.000003	5.843 ***
s	0.001344	1.7 *		

Ficticious Solution Standard Deviation and Percent Error (cont.)

Variable	Lens and Projective		Lens and Electronic	
	Std. Dev.	% Error	Std. Dev.	% Error
l1	0.0	0.037	0.0	0.009
l2	0.0	0.0	0.0	0.0
q1	0.0	0.095 *	0.0	0.011
q2	0.0	0.093 *	0.0	0.032
θ	0.000038	0.003	0.000058	0.001
a1	0.0	0.009	0.0	0.033
a2	0.0	0.017	0.0	0.053
K	0.000001	0.066 *		
ϕ	0.0	0.003		
w	0.0	0.001		
Xo	0.000013	-0.00001		
Yo	0.000013	0.0		
Zo	0.000024	0.0		
d			0.0	0.0
e			0.0	0.002
h			0.000011	0.027
k			0.0	0.005
n			0.0	0.007
s			0.00001	0.036

Ficticious Solution Standard Deviation and Percent Error (cont.)

Variable	Electronic Distortion Solution	
	Std. Dev.	% Error
d	0.0	0.001
e	0.0	0.009
h	0.000006	0.014
k	0.0	0.0
n	0.0	0.011
s	0.000006	0.002

values for each method. An "****" indicates those errors which, if taken alone, would cause an error of at least 1 micron if x = 30mm and y = 30mm. An error value accompanied by "**" indicates an approximation which would cause more than a 0.1 micron error in adjusted coordinates.

Five unknowns in the 19 parameter solution and three from the lens-orientation routine were inaccurate enough to produce a 0.1 micron error. In addition, eight more of the 17 parameters were sufficiently imprecise to cause 1.0 micron errors.

The 17 parameter method was identical to the 19 unknown solution attempt except that the constant term in the x and y compression distortion formulae were dropped. When the 19 parameter results were obtained, some covariance between Xo and h and the Yo and s was observed, indicating that some dependence existed. Their respective variances were approximately equal also. In an attempt to eliminate the dependence the 17 parameter formulae were created by omission of the two coefficients. Any difference observed between the four remaining ficticious

solutions are insignificant. The 17 element solution was dropped after the ficticious processing and was not used in the subsequent analysis of real measurements. The relative success of the real data results illustrated the comparative effectiveness of the other four procedures used.

Real Data Testing

The five measurement sets were used as input for the four distortion analysis procedures. The original raw input coordinates were rectified by an affine transformation as a tertiary treatment which would be routine. The affine transformation had mean residuals as shown below remaining:

Affine Transformation Residuals

Measurement Set	Mean Residuals (Scaled to 10 mm spacing) x, mm	y, mm
1	0.1414	0.5476
2	0.2306	0.8605
3	0.1431	0.7167
4	0.2353	0.6654
5	0.2035	1.6161

The principal results of the 20 determinations are given in the next table, including percent improvement of the mean coordinates. Comparison of the values must be made with respect to the scale of the grid which is represented by its interval spacing. Between solution types the final SSR and mean residuals can be related with respect to the scale. All twenty pairs of scaled residuals and percent improvement can be compared directly.

Distortion Analysis Results from Real Data

Meas. Set	Solution Type Used	Grid Int.	Final SSR	Residuals Scaled to 10 mm x, mm	y,mm	Mean Residual % Improvement x	y
1	(19) Lens,	5	6.00	0.134	0.504	15.1	7.9
2		10	60.87	0.196	0.770	15.2	10.5
4	Projective	10	38.85	0.151	0.562	35.7	15.5
3		15	82.10	0.110	0.714	23.3	0.3
5	Electronic	15	153.10	0.195	0.938	-43.0	13.0
1		5	7.02	0.129	0.523	8.9	4.5
2	(13) Lens,	10	72.72	0.223	0.856	3.3	4.8
4		10	49.45	0.202	0.658	14.1	1.1
3	Projective	15	95.42	0.129	0.750	10.0	-4.7
5		15	203.34	0.217	1.056	-60.0	1.9
1		5	6.91	0.128	0.523	8.9	4.5
2	(13) Lens,	10	65.41	0.234	0.768	3.0	10.8
4		10	45.63	0.216	0.619	8.1	7.0
3	Electronic	15	83.01	0.134	0.690	6.3	3.7
5		15	209.93	0.193	1.079	-42.1	-0.2
1		5	6.89	0.152	0.528	-7.5	3.6
2	(6)	10	64.38	0.232	0.782	-0.8	9.1
4	Electronic	10	45.05	0.236	0.605	-0.4	9.0
3		15	85.46	0.140	0.700	2.0	2.3
5		15	225.62	0.133	1.105	1.6	-2.6

All the data sets allowed for a convergent solution in the four procedures. For each measurement set the sum of squared residuals was smallest in the complete solution containing all variables and indicates a higher degree of stability of that procedure.

The fourth data set displayed the most consistent and highest improvement with all distortion types. The coordinates of set five became worse in almost every instance, although the standard deviation of the solved for coefficients was smaller in

solutions are insignificant. The 17 element solution was dropped after the ficticious processing and was not used in the subsequent analysis of real measurements. The relative success of the real data results illustrated the comparative effectiveness of the other four procedures used.

Real Data Testing

The five measurement sets were used as input for the four distortion analysis procedures. The original raw input coordinates were rectified by an affine transformation as a tertiary treatment which would be routine. The affine transformation had mean residuals as shown below remaining:

Affine Transformation Residuals

Measurement Set	Mean Residuals (Scaled to 10 mm spacing) x, mm	y, mm
1	0.1414	0.5476
2	0.2306	0.8605
3	0.1431	0.7167
4	0.2353	0.6654
5	0.2035	1.6161

The principal results of the 20 determinations are given in the next table, including percent improvement of the mean coordinates. Comparison of the values must be made with respect to the scale of the grid which is represented by its interval spacing. Between solution types the final SSR and mean residuals can be related with respect to the scale. All twenty pairs of scaled residuals and percent improvement can be compared directly.

Distortion Analysis Results from Real Data

Meas. Set	Solution Type Used	Grid Int.	Final SSR	Residuals Scaled to 10 mm x, mm	y,mm	Mean Residual % Improvement x	y
1	(19) Lens,	5	6.00	0.134	0.504	15.1	7.9
2		10	60.87	0.196	0.770	15.2	10.5
4	Projective	10	38.85	0.151	0.562	35.7	15.5
3		15	82.10	0.110	0.714	23.3	0.3
5	Electronic	15	153.10	0.195	0.938	-43.0	13.0
1		5	7.02	0.129	0.523	8.9	4.5
2	(13) Lens,	10	72.72	0.223	0.856	3.3	4.8
4		10	49.45	0.202	0.658	14.1	1.1
3	Projective	15	95.42	0.129	0.750	10.0	-4.7
5		15	203.34	0.217	1.056	-60.0	1.9
1		5	6.91	0.128	0.523	8.9	4.5
2	(13) Lens,	10	65.41	0.234	0.768	3.0	10.8
4		10	45.63	0.216	0.619	8.1	7.0
3	Electronic	15	83.01	0.134	0.690	6.3	3.7
5		15	209.93	0.193	1.079	-42.1	-0.2
1		5	6.89	0.152	0.528	-7.5	3.6
2	(6)	10	64.38	0.232	0.782	-0.8	9.1
4	Electronic	10	45.05	0.236	0.605	-0.4	9.0
3		15	85.46	0.140	0.700	2.0	2.3
5		15	225.62	0.133	1.105	1.6	-2.6

All the data sets allowed for a convergent solution in the four procedures. For each measurement set the sum of squared residuals was smallest in the complete solution containing all variables and indicates a higher degree of stability of that procedure.

The fourth data set displayed the most consistent and highest improvement with all distortion types. The coordinates of set five became worse in almost every instance, although the standard deviation of the solved for coefficients was smaller in

measurement set five in nearly every case. The results from the other three sets showed little improvement in residual error.

Results of the fourth data set analysis by the full 19 parameter procedure provided the highest percent coordinate improvement. The distortion vectors which were found are given in the following four figures.

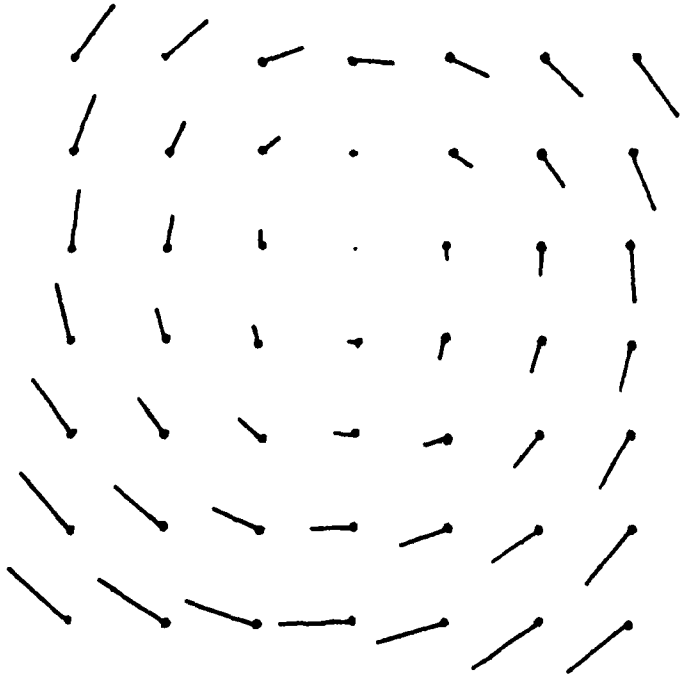

Combined Lens Distortion Vectors. ⟷ = 2 mm.

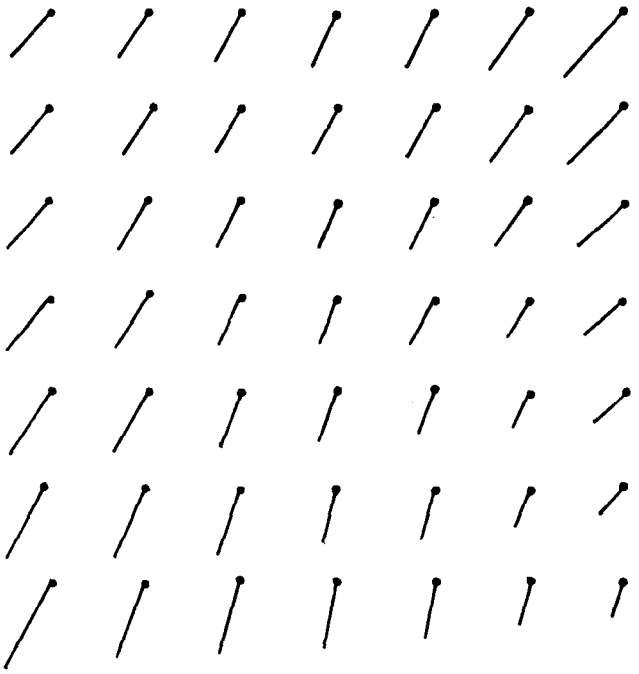

Orientation Adjustment Vectors. ⟷ = 20 mm.

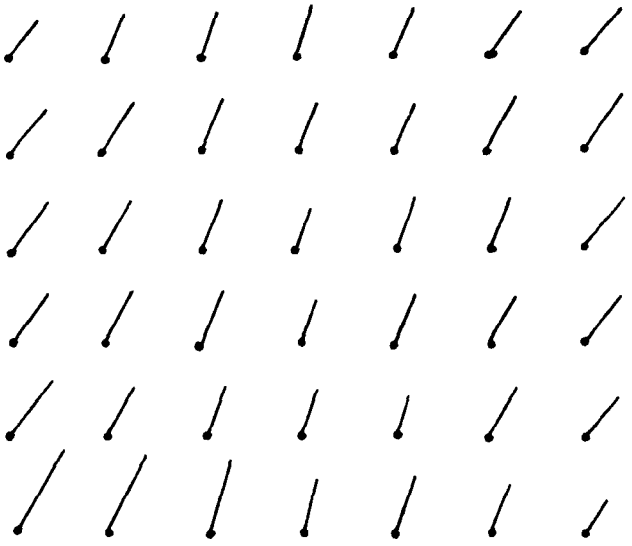

Electronic Distortion Vectors. ⟷ = 20 mm.

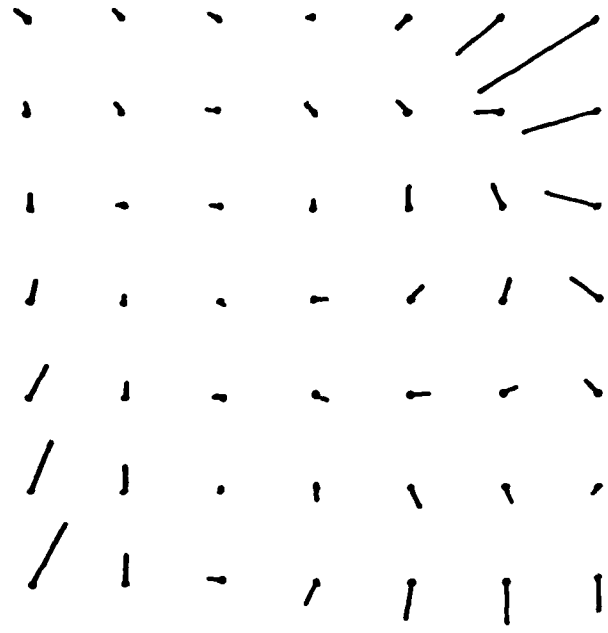

Total Removed Distortions. ⟷ = 1.6 mm.

The average absolute magnitudes for each type of distortion in x and y are shown below.

Mean Distortions Removed

Distortion	Mean x Magnitude, mm	Mean y Magnitude, mm
Symmetric Radial	0.011	0.013
Symmetric Tangential	0.642	0.610
Asymmetric	0.033	0.040
Orientation	5.223	10.350
Trapezoidal	0.838	1.499
Compression	5.400	10.370
TOTAL	0.2545	0.2761

Analysis of Significant Factors

The null hypothesis for the ANOVA computations states that no difference exists between the factors and their interactions. If significance is found it indicates a situation justifying a rejection of the hypothesis.

Particular observations within a treatment combination are assumed to show only chance variation since they were all treated equally. Observations of different treatments within a level differ due to the effect of the treatment combination plus the variability within the level.

Under the assumptions made for multi-factor ANOVA, the sum of squares for levels and treatments are independent. The F tests themselves, however, are not. There is some dependency between them due to their use of a common denominator. For 14 F tests, there is a small probability that one will show a false significance at the 0.05 level and a little chance that one will be falsely significant at the 0.01 confidence level.

All 245 point measurements of 9 pointings each in x and y were used to compute 490 variance values which were then transformed by log 10 for the ANOVA routine. The 490 observations were partitioned into 4 levels: two coordinates; seven columns; seven rows; and five data sets or setups. A full ANOVA table was computed and follows. There was one observation per combination so the sum of squares error was taken as the treatment containing all levels. All F ratios were computed and tested at the 0.05 and 0.01 level. Eight of the fifteen levels and interaction effects were found to be significant at 0.05 and seven were found at the 0.01 level.

Four Factor ANOVA Table

Factors	Source	Sum of Squares	DF	Mean Square	F Ratio	Sig. at 1%	Sig. at 5%	Signif. Diff.
Coordinates	A	120.152	1	120.125	1486.10	X	X	0.067
Columns	B	1.112	6	0.1853	2.292		X	0.125
Rows	C	6.334	6	1.0566	13.07	X	X	0.125
Setups	D	2.020	4	0.5051	6.247	X	X	0.106
	AB	0.664	6	0.1107	1.369	X	X	0.177
	AC	6.503	6	1.0838	13.41			0.177
	AD	8.047	4	2.0118	24.88	X	X	0.150
	BC	5.543	36	0.1540	1.905	X	X	0.332
	BD	1.849	24	0.0770	0.953	X	X	0.280
	CD	2.886	24	0.1203	1.488			0.280
	ABC	3.333	36	0.0926	1.145			0.469
	ABD	1.964	24	0.0818	1.012			0.397
	ACD	1.699	24	0.0708	0.876			0.397
	BCD	20.470	144	0.1422	1.758	X	X	0.742
Error	REM	11.647	144	0.080851				
TOTAL	SST	194.2266	489	0.397191				

To test the interaction combinations within each treatment, a multiple range test was used for comparison of consecutive means at a 0.01 confidence level. The significance test for the first four levels is shown below. A line connects those means which do not differ significantly. The other level means for the interaction and the significant difference test are only valid for those levels already found to be different from the F tests.

Factor A, coordinate type, contained a very high degree of significant difference, as expected. More than 14 significant intervals were found to exist between the x and y coordinate level means. A large amount of overlap is present in the two intervals containing the levels means for columns which had been significant at the 0.05 level only. The increased variability of the column level illustrates the variance of the y coordinates.

Significant Intervals of Main Factors

Coordinates A		Columns B		Rows C		Setups D	
1	0.48045	5	1.08018	5	1.10064	3	1.05787
2	1.47082	6	0.98380	7	1.09607	1	1.00845
		7	0.97838	6	1.07634	4	0.98988
		4	0.96959	3	1.00271	2	0.95687
		1	0.95907	4	0.89684	5	0.86509
		2	0.94052	2	0.82893		
		3	0.91790	1	0.82788		

All the treatments which contained coordinate type as a factor were completely separated into their x and y components. The x half of the AB, AC, AD, ABC, ABD and ACD levels always differed by less than the y half and always spanned a smaller number of intervals.

Results of the significance tests for the other combinations follow.

Coordinates - Columns	A	B	
	2	5	1.59844
	2	4	1.48977
	2	1	1.48741
	2	2	1.47459
	2	6	1.43064
	2	7	1.41755
	2	3	1.39734
	1	5	0.56192
	1	7	0.53921
	1	6	0.53695
	1	4	0.44941
	1	3	0.43846
	1	1	0.43073
	1	2	0.40646

Coordinates - Rows	A	C	
	2	7	1.72632
	2	5	1.71595
	2	6	1.66169
	2	3	1.50137
	2	4	1.34485
	2	2	1.22003
	2	1	1.12552
	1	1	0.53025
	1	3	0.50406
	1	6	0.49100
	1	5	0.48532
	1	7	0.46583
	1	4	0.44884
	1	2	0.43783

Coordinates -Setups	A	D	
	2	3	1.67489
	2	2	1.56244
	2	1	1.54877
	2	4	1.43181
	2	5	1.13619
	1	5	0.59399
	1	4	0.54795
	1	1	0.46814
	1	3	0.44085
	1	2	0.35130

Columns - Rows	B	C	
	6	7	1.32168
	5	5	1.32041
	3	5	1.25918
	1	7	1.24199
	2	5	1.23628
	4	6	1.21859
	4	7	1.15388
	5	6	1.15192
	7	3	1.14786
	7	6	1.13841
	5	4	1.13019
	1	6	1.09188
	5	3	1.06566
	6	6	1.06186
	7	5	1.04442
	2	7	1.03820
	3	7	1.03271
	5	7	1.02852
	2	3	1.02386
	4	3	1.00873
	4	5	1.00416
	6	1	0.99913
	2	6	0.98228
	7	2	0.97675
	1	3	0.97085
	5	1	0.94941
	6	5	0.94184
	3	4	0.91595
	5	2	0.91513
	3	3	0.90147
	1	2	0.90058
	6	3	0.90057
	1	5	0.89818
	4	4	0.89469
	3	6	0.88947
	2	4	0.88025
	7	1	0.86858
	6	2	0.86824
	7	7	0.85554
	1	4	0.84647
	7	4	0.81710
	6	4	0.79326
	4	2	0.76390
	1	1	0.76352
	2	1	0.74316
	4	1	0.74316

	3	1	0.72823
	3	2	0.69830
	2	2	0.67963

Columns - Setups	B	D	
	5	1	1.18724
	1	3	1.14589
	2	3	1.13649
	5	4	1.13501
	5	3	1.06957
	5	2	1.06629
	6	3	1.05130
	4	1	1.04669
	4	2	1.04362
	4	3	1.04345
	7	1	1.01800
	6	1	1.01745
	7	4	0.99979
	3	3	0.99588
	2	4	0.99400
	1	4	0.99374
	2	1	0.98115
	1	2	0.97881
	7	2	0.96636
	7	3	0.96251
	6	5	0.95857
	6	4	0.94641
	6	2	0.94526
	7	5	0.94523
	4	4	0.94402
	5	5	0.94278
	1	1	0.92000
	3	4	0.91619
	3	5	0.90395
	3	1	0.88864
	3	2	0.88484
	2	2	0.81294
	2	5	0.77804
	4	5	0.77016
	1	5	0.75691

Rows - Setups

C	D	
7	3	1.28424
6	3	1.25035
6	4	1.21756
7	2	1.18851
5	3	1.17154
5	1	1.13675
5	4	1.11531
5	2	1.11435
6	1	1.11136
3	3	1.10887
7	4	1.10882
4	1	1.04508
3	1	1.00916
6	2	0.99179
3	4	0.98359
7	1	0.97861
3	2	0.97022
2	1	0.96939
5	5	0.96524
4	3	0.95944
3	5	0.94174
7	5	0.92019
1	4	0.90309
4	2	0.87858
1	5	0.87617
2	3	0.86119
4	4	0.82864
6	5	0.81067
1	1	0.80883
1	2	0.781 6
2	2	0.772 1
4	5	0.77249
2	4	0.77216
1	3	0.76947
2	5	0.76913

Coordinates
Columns - Rows

A	B	C	
2	5	5	2.11270
2	1	7	2.07958
2	6	7	2.05146
2	2	5	2.02316
2	3	5	1.94350
2	4	6	1.90702
2	4	7	1.79614
2	5	6	1.74948
2	1	6	1.73190

2 2 7	1.68432
2 7 6	1.67926
2 7 3	1.67394
2 3 7	1.67280
2 2 3	1.62682
2 5 4	1.62448
2 4 5	1.61374
2 1 3	1.59390
2 2 6	1.55518
2 5 3	1.54894
2 6 6	1.53798
2 7 5	1.53016
2 5 7	1.47192
2 3 6	1.47102
2 4 3	1.45630
2 2 4	1.41954
2 6 5	1.41754
2 4 4	1.39214
2 5 2	1.38576
2 7 2	1.37636
2 3 4	1.37532
2 1 5	1.37088
2 1 2	1.34458
2 6 2	1.33130
2 7 7	1.32800
2 3 3	1.31280
2 6 3	1.29690
2 5 1	1.29578
2 1 4	1.29170
2 6 1	1.25892
2 7 4	1.19036
2 7 1	1.14478
2 4 2	1.13214
2 4 1	1.13090
2 6 4	1.12040
2 3 1	1.05248
2 2 2	1.01662
2 1 1	0.99932
2 2 1	0.99646
2 3 2	0.95346
1 6 1	0.73934
1 5 4	0.63590
1 7 3	0.62178
1 5 1	0.60304
1 7 6	0.59756
1 7 1	0.59238
1 6 7	0.59190

1 6 6	0.58574
1 5 7	0.58512
1 5 3	0.58238
1 7 2	0.57714
1 3 5	0.57486
1 4 3	0.56116
1 7 5	0.55868
1 5 6	0.55436
1 4 6	0.53016
1 5 5	0.52812
1 1 1	0.52772
1 4 7	0.51162
1 6 3	0.50424
1 3 3	0.49014
1 2 1	0.48986
1 6 5	0.46614
1 6 4	0.46612
1 1 2	0.45658
1 3 4	0.45658
1 1 6	0.45186
1 2 5	0.44940
1 5 2	0.44450
1 7 4	0.44384
1 3 2	0.44314
1 1 5	0.42548
1 2 3	0.42090
1 2 6	0.40938
1 6 2	0.40518
1 1 7	0.40440
1 3 1	0.40398
1 1 4	0.40124
1 4 4	0.39724
1 4 2	0.39566
1 4 5	0.39458
1 3 7	0.39262
1 2 7	0.39208
1 7 7	0.38308
1 4 1	0.35542
1 1 3	0.34780
1 2 2	0.34264
1 2 4	0.34096
1 3 6	0.30792

Coordinates Columns - Setups	A	B	D	
	2	2	3	1.92534
	2	1	3	1.82566
	2	4	2	1.75703
	2	5	3	1.73869
	2	5	1	1.73430
	2	4	3	1.69496
	2	4	1	1.67411
	2	5	2	1.65309
	2	1	2	1.62764
	2	2	1	1.61960
	2	5	4	1.57074
	2	7	2	1.56740
	2	3	3	1.55723
	2	6	3	1.53191
	2	1	4	1.52659
	2	6	2	1.49803
	2	1	1	1.49659
	2	3	2	1.48646
	2	7	1	1.48030
	2	2	4	1.47614
	2	6	1	1.46997
	2	7	3	1.45044
	2	4	4	1.38946
	2	3	4	1.36764
	2	3	1	1.36650
	2	7	4	1.35543
	2	2	2	1.34746
	2	6	4	1.33666
	2	6	5	1.31664
	2	5	5	1.29537
	2	7	5	1.23419
	2	3	5	1.20887
	2	2	5	1.00439
	2	1	5	0.96057
	2	4	5	0.93329
	1	5	4	0.69927
	1	7	5	0.65627
	1	7	4	0.64416
	1	5	1	0.64019
	1	4	5	0.60703
	1	6	5	0.60050
	1	3	5	0.59903
	1	5	5	0.59019
	1	6	3	0.57069
	1	6	1	0.56493
	1	6	4	0.55616

1	7	1	0.55570
1	1	5	0.55324
1	2	5	0.55169
1	2	4	0.51186
1	4	4	0.49859
1	5	2	0.47949
1	7	3	0.47459
1	1	3	0.46611
1	3	4	0.46474
1	1	4	0.46089
1	3	3	0.43453
1	4	1	0.41926
1	3	1	0.41079
1	5	3	0.40046
1	6	2	0.39249
1	4	3	0.39194
1	7	2	0.36533
1	2	3	0.34764
1	1	1	0.34341
1	2	1	0.34270
1	4	2	0.33021
1	1	2	0.32997
1	3	2	0.28323
1	2	2	0.27841

Coordinates - Rows - Setups

A	C	D	
2	7	3	2.07384
2	6	3	1.98493
2	5	3	1.97500
2	7	2	1.96914
2	6	4	1.84874
2	5	2	1.84623
2	3	3	1.81969
2	5	1	1.79673
2	6	1	1.77147
2	7	4	1.73274
2	4	1	1.65287
2	5	4	1.62597
2	6	2	1.61046
2	7	1	1.60047
2	3	2	1.55371
2	3	1	1.44947
2	4	2	1.42966
2	3	4	1.41537
2	2	1	1.40877
2	4	3	1.40564
2	2	3	1.36744

2	5	5	1.33584
2	2	2	1.30323
2	3	5	1.26861
2	7	5	1.25539
2	4	4	1.23759
2	1	2	1.22467
2	1	1	1.16159
2	1	4	1.14463
2	1	3	1.09769
2	6	5	1.09286
2	2	4	1.01761
2	2	5	1.00310
2	1	5	0.99903
2	4	5	0.99849
1	1	5	0.75331
1	1	4	0.66154
1	3	5	0.61486
1	5	4	0.60466
1	5	5	0.59464
1	6	4	0.58637
1	7	5	0.58499
1	3	1	0.56884
1	3	4	0.55180
1	4	5	0.54650
1	2	5	0.53516
1	2	1	0.53000
1	6	5	0.52849
1	2	4	0.52670
1	6	3	0.51577
1	4	3	0.51323
1	7	3	0.49464
1	7	4	0.48490
1	5	1	0.47677
1	1	1	0.45607
1	6	1	0.45124
1	1	3	0.44126
1	4	1	0.43729
1	4	4	0.41969
1	7	2	0.40787
1	3	3	0.39806
1	3	2	0.38673
1	5	2	0.38247
1	6	2	0.37311
1	5	3	0.36807
1	7	1	0.35676
1	2	3	0.35493
1	1	2	0.33906

	1	4	2	0.32750
	1	2	2	0.24239

Columns - Rows - Setups	B	C	D	
	7	6	4	1.75645
	5	5	4	1.75080
	1	7	4	1.74635
	6	7	4	1.74485
	5	4	2	1.66415
	5	5	1	1.66085
	4	6	3	1.64260
	1	5	3	1.60085
	2	6	4	1.57550
	3	5	2	1.55080
	4	7	2	1.55005
	5	4	1	1.53165
	2	7	3	1.52560
	7	6	3	1.52085
	1	6	2	1.49605
	2	5	3	1.47105
	4	6	1	1.47100
	5	7	3	1.46535
	2	5	4	1.45690
	6	6	2	1.44905
	6	7	2	1.39785
	7	5	2	1.38510
	3	5	4	1.38450
	5	6	3	1.38030
	5	3	2	1.37380
	5	1	1	1.37285
	6	2	1	1.37035
	1	6	4	1.36130
	5	6	4	1.36045
	1	7	3	1.35885
	6	7	3	1.34160
	1	2	3	1.33705
	1	7	2	1.32920
	6	6	3	1.32820
	4	2	1	1.32070
	2	7	1	1.31925
	5	1	4	1.31760
	7	3	1	1.31300
	3	4	3	1.29600
	6	3	1	1.29210
	5	6	5	1.28195
	4	3	4	1.25870
	6	1	3	1.24735

5	7	2	1.24060
1	3	2	1.23970
2	5	1	1.23125
7	3	3	1.22795
6	7	5	1.22615
4	7	3	1.22440
4	6	2	1.22185
3	6	1	1.22175
2	4	3	1.22010
1	3	3	1.19895
2	3	3	1.19895
7	2	1	1.19380
3	7	3	1.18875
4	5	1	1.18475
2	3	2	1.17340
5	3	5	1.17005
5	5	3	1.17000
6	5	5	1.16875
6	1	4	1.16805
3	5	1	1.16440
2	4	1	1.16295
1	6	1	1.15830
5	6	1	1.15455
4	3	3	1.13910
7	5	5	1.12985
5	3	4	1.12750
3	3	5	1.12495
4	5	3	1.11095
7	3	5	1.10655
7	7	2	1.10455
6	1	5	1.10230
3	7	5	1.10105
3	5	5	1.09880
3	5	3	1.09740
3	3	3	1.09500
5	2	3	1.08985
7	1	5	1.08545
5	5	2	1.07745
2	5	2	1.07585
4	7	4	1.07515
4	4	3	1.06940
2	6	1	1.06895
2	6	3	1.06185
4	5	2	1.05755
7	3	4	1.05465
7	2	4	1.04230
7	4	1	1.04165

7	3	2	1.03715
6	5	3	1.03565
7	5	1	1.02940
6	5	2	1.02940
6	4	1	1.02575
2	3	4	1.01485
5	7	1	1.01195
4	6	5	1.01005
1	3	1	1.00405
6	3	3	1.00160
7	4	5	1.00045
3	7	4	0.99180
4	7	1	0.97595
4	5	4	0.97315
1	4	3	0.96920
7	5	4	0.96290
4	1	4	0.96175
3	4	4	0.96175
4	4	2	0.95340
3	7	1	0.95155
2	5	5	0.94635
1	7	5	0.94635
4	7	5	0.94385
5	5	5	0.94295
1	4	1	0.94150
5	2	5	0.93555
6	5	1	0.93370
7	1	2	0.93040
3	7	2	0.93040
6	3	4	0.92685
1	1	5	0.92565
5	4	5	0.92295
3	3	1	0.91970
4	4	4	0.91280
1	6	3	0.91145
6	6	4	0.90830
3	6	3	0.90720
4	3	5	0.90590
1	1	1	0.90455
4	3	1	0.90300
5	3	3	0.90055
6	7	1	0.89795
7	2	5	0.89110
3	1	2	0.88660
7	7	3	0.88515
2	4	4	0.88515
6	4	5	0.88475

7	2	2	0.87845
7	2	3	0.87810
2	3	1	0.87585
2	1	3	0.87050
5	2	2	0.86640
7	6	2	0.86525
4	1	2	0.86505
7	7	1	0.86445
5	2	4	0.86140
3	6	2	0.85945
2	3	5	0.85625
6	6	1	0.85455
1	2	4	0.85315
7	6	1	0.85040
1	2	1	0.84950
2	7	5	0.84130
4	3	2	0.83695
2	2	5	0.83580
2	1	5	0.83510
3	1	5	0.83415
3	2	3	0.83355
7	1	1	0.83330
1	4	4	0.83270
4	4	1	0.83215
1	7	1	0.82920
5	2	1	0.82245
4	2	2	0.82050
6	2	5	0.81710
3	6	4	0.81345
3	4	2	0.80170
1	2	2	0.78980
3	2	5	0.78280
5	4	4	0.78110
3	4	1	0.77990
3	3	4	0.77770
1	5	5	0.77560
7	1	3	0.77380
6	2	2	0.77140
6	6	5	0.76920
2	7	2	0.76690
2	1	2	0.75955
1	4	5	0.75835
5	3	1	0.75640
1	5	1	0.75290
5	4	3	0.75110
6	1	1	0.74775
4	6	4	0.74745

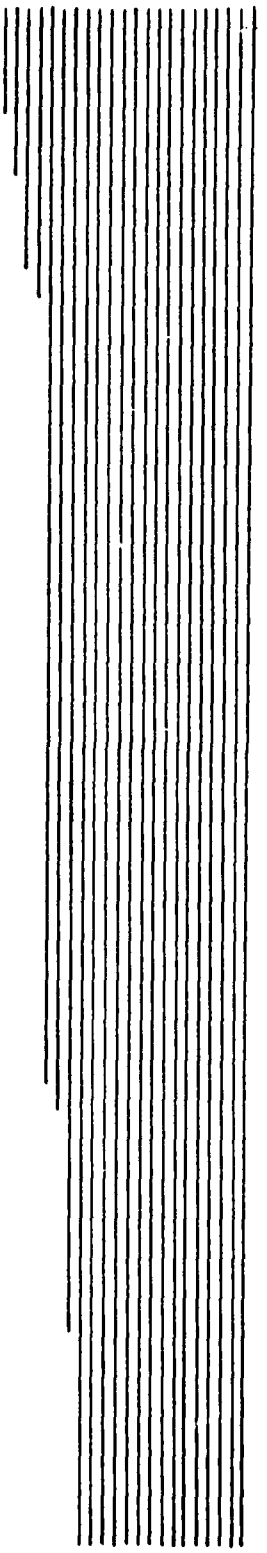

5 7 4	0.74620
3 1 4	0.74400
7 4 4	0.74285
6 3 5	0.74175
3 4 5	0.74040
3 2 4	0.74015
2 4 2	0.73820
2 7 4	0.73795
1 5 4	0.73725
7 4 3	0.73690
2 6 5	0.73660
6 2 3	0.73135
1 4 2	0.73060
6 1 2	0.73020
5 1 3	0.72985
1 3 4	0.72485
7 1 4	0.71995
7 7 4	0.71945
7 5 3	0.71485
2 1 4	0.70970
2 2 2	0.70815
4 4 5	0.70570
7 7 5	0.70410
1 1 4	0.70055
7 6 5	0.69910
6 4 2	0.69835
4 5 5	0.69440
1 3 5	0.68670
6 4 4	0.68410
4 1 5	0.68305
4 2 4	0.67915
5 7 5	0.67850
1 2 5	0.67340
6 4 3	0.67335
2 2 1	0.66885
5 1 5	0.66750
5 1 2	0.65925
6 2 4	0.65100
3 6 5	0.64550
1 1 3	0.64485
1 1 2	0.64200
4 1 1	0.63925
1 5 2	0.62430
3 1 1	0.62315
2 2 3	0.60740
3 3 2	0.59000
5 6 2	0.58235

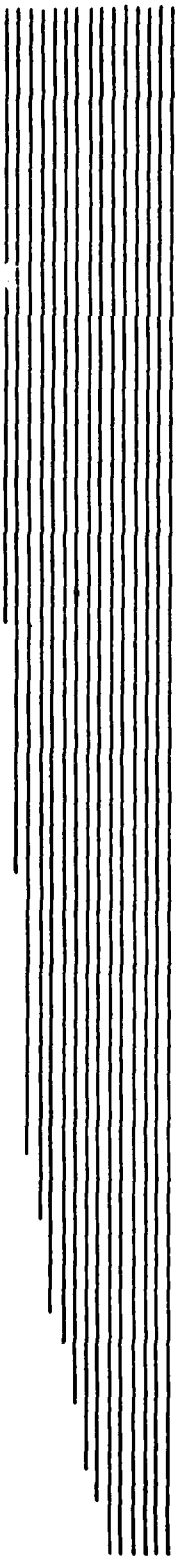

2 2 4	0.57795
3 2 2	0.57495
4 1 3	0.56670
7 4 2	0.56365
3 2 1	0.56005
3 1 3	0.55325
4 2 3	0.55100
6 5 4	0.54170
2 1 1	0.54095
6 3 2	0.54055
1 6 5	0.53230
2 6 2	0.46850
4 2 5	0.44815
2 4 5	0.39485

CONCLUSIONS / SUMMARY

An analytical photogrammetric procedure was developed and tested in an attempt to define a mathematical method for precisely measuring television camera position, attitude and image distortion through mensuration of a calibrated grid viewed through the system.

The similarities between frame photographic camera geometry and television camera geometry allowed analytical photogrammetric principles to be applied to the problem of calibrating images displayed on CRT devices. Additional mathematical expressions were implemented to model distortions particular to the nature of TV cameras and display systems.

Mathematical formulae describing the geometric affects of camera location and attitude, lens distortion and electronic distortions were combined in a least squares numerical solution. Preliminary testing provided assurance that the formulae and computer implementation were correct before the performance of one simultaneous solution combining all the image distortion formulae. Any remaining errors in image geometry were then attributed to mensuration errors and/or interaction between the distortion models. Both did contribute significant error in the reduction of real data.

The figures on page 6 illustrate the similarity of several combinations of possible image distortion. The very significant interaction between camera position and electronic distortion is illustrated on page 31 where orientation and position residuals are nearly equal and opposite to those for electronic distortion. This indicates the very nearly indeterminate solution caused by

the interaction.

A multiple range test was performed on the raw measurment data as well. In an effort to identify sources of mensuration error, levels of coordinate type, point placement and measurement sets were compared. The variances of coordinate levels x and y were very significantly different. The high variability of y coordinate measurements and measurment error did significantly degrade the results. There was some difference in the accuracy obtainable between the lower half and upper half of the display. Approximately 81% of the points located within the bottom 3/7 of the display had a higher position mensuration variance than the other points.

The mathematical formulation of the various error types can be used to determine the respective errors completely, but not in a single simultaneous solution. Independent determinations of electronic distortion and camera position must be used and coordinate mensuration errors should be monitored and minimized.

From the significant difference analysis it is also clear that the variability of the y variance itself is typically larger. Any differences among the other levels and interactions is either small in comparison to, or may be directly affected by the y coordinate measurement variance.